Geophysical Research Letters

RESEARCH LETTER
10.1029/2024GL108334

Assessment of the Origin of a Plasma Depletion Band Over the United States During the 8 September 2017 Geomagnetic Storm

Hyosub Kil[1], Andrew K. Sun[2], Woo Kyoung Lee[3,4], Hyeyeon Chang[5], and Jiyun Lee[2]

[1]The Johns Hopkins University Applied Physics Laboratory, Laurel, MD, USA, [2]Department of Aerospace Engineering, Korea Advanced Institute of Science and Technology, Daejeon, Republic of Korea, [3]Korea Astronomy and Space Science Institute, Daejeon, Republic of Korea, [4]Korea University of Science and Technology, Daejeon, Republic of Korea, [5]Ann and H. J. Smead Aerospace Engineering Sciences Department, University of Colorado at Boulder, Boulder, CO, USA

Key Points:

- A new perspective on the interpretation of a plasma depletion band over the United States during the 8 September 2017 storm is presented
- Equatorial plasma bubble (EPB) was proposed as its source in previous studies, but we report non-EPB characteristics in this phenomenon
- Considering its emergence time, location relative to EPB, and intensification with time, this event can be a local midlatitude phenomenon

Correspondence to:
H. Kil,
hyosub.kil@jhuapl.edu

Citation:
Kil, H., Sun, A. K., Lee, W. K., Chang, H., & Lee, J. (2024). Assessment of the origin of a plasma depletion band over the United States during the 8 September 2017 geomagnetic storm. *Geophysical Research Letters*, *51*, e2024GL108334. https://doi.org/10.1029/2024GL108334

Received 14 JAN 2024
Accepted 16 MAR 2024

Author Contributions:
Conceptualization: Hyosub Kil, Woo Kyoung Lee
Data curation: Andrew K. Sun
Formal analysis: Andrew K. Sun, Hyeyeon Chang
Funding acquisition: Hyosub Kil, Jiyun Lee
Investigation: Andrew K. Sun
Methodology: Hyosub Kil, Woo Kyoung Lee, Hyeyeon Chang
Software: Andrew K. Sun
Supervision: Hyosub Kil, Jiyun Lee
Validation: Hyosub Kil, Woo Kyoung Lee, Hyeyeon Chang
Visualization: Andrew K. Sun
Writing – original draft: Hyosub Kil
Writing – review & editing: Andrew K. Sun, Woo Kyoung Lee

Abstract The development of an intense total electron content (TEC) depletion band over the United States during the 8 September 2017 geomagnetic storm was understood as the extension of an equatorial plasma bubble (EPB) to midlatitudes in previous studies. However, this study reports non-EPB aspects within this phenomenon. First, the simultaneous emergence of the TEC depletion band at midlatitudes and EPBs in the equatorial region indicates that the midlatitude TEC depletion band is not initiated by an EPB. Second, the intensification of TEC depletion at midlatitudes during the decay of TEC depletion at intermediate latitudes is anomalous. Third, the location of the TEC depletion band at midlatitudes is inconsistent with the EPB location estimated from zonal plasma motion. Given ionospheric perturbations in North America from the beginning of the storm, it is plausible that the TEC depletion band was locally generated in association with these perturbations.

Plain Language Summary Intense plasma depletions occasionally occur at midlatitudes during geomagnetic storms. Due to their morphological similarity to plasma bubbles that develop in the equatorial region, midlatitude depletions are often considered extensions of equatorial plasma bubbles (EPBs) to midlatitudes. However, midlatitude depletions are also recognized as locally generated phenomena. During the 8 September 2017 geomagnetic storm, an anomalously large total electron content (TEC) depletion band emerged in TEC maps over the American sector. This feature appears as a single structure, extending from the equatorial region to midlatitudes in both hemispheres. While this phenomenon is commonly understood as the extension of an EPB to midlatitudes, this study reports non-EPB aspects that were not discussed in previous studies.

1. Introduction

An intense total electron content (TEC) depletion band was detected over the United States (US) during the geomagnetic storm on 8 September 2017. The TEC depletion band spans several hundred kilometers in width and extends thousands of kilometers across the US. The combination of this TEC depletion band with an equatorial plasma bubble (EPB) feature near the magnetic equator creates a backward (inverted or reversed) "C"-shaped structure, resembling the morphology of an EPB. In addition to this morphological similarity, the apparent poleward propagation of density perturbations and the detection of a conjugate depletion at southern midlatitudes have led to the interpretation of the entire backward C-shaped structure in terms of an EPB (Aa et al., 2019; Zakharenkova & Cherniak, 2020). This interpretation aligns with the understanding of large midlatitude plasma depletions during geomagnetic storms as signatures of EPBs (Aa et al., 2018; Cherniak & Zakharenkova, 2016, 2022; Cherniak et al., 2019; Huang et al., 2007; Ma & Maruyama, 2006; Martinis et al., 2015).

However, uncertainties remain in the interpretation of the backward C-shaped TEC depletion structure on 8 September 2017 in terms of EPB. Ionospheric perturbations existed over the US before the development of EPBs in the equatorial region. Therefore, it is challenging to distinguish locally generated midlatitude perturbations from those originating in the equatorial region. The emergence time, evolution across different latitudes, and tilt of the structure provide valuable insight for assessing its connection to EPB (Kil et al., 2016), but these aspects of the 8 September 2017 event have not been addressed in prior studies. In the study of Nishimura et al. (2021), the TEC depletion band over the US on 8 September 2017 was interpreted as a structure that developed between

storm enhanced density (SED) features, indicating the generation of gradient drift instability at the edge of SEDs. This interpretation is aligned with the understanding of midlatitude plasma depletions as local midlatitude phenomena (Chang et al., 2022; Kil et al., 2016, 2022; Nishioka et al., 2009; Sahai et al., 2001; Sun et al., 2013).

The TEC depletion band on 8 September 2017 represents a rare event, the evolution of which from the equatorial region to midlatitudes is traceable using Global Navigation Satellite System (GNSS) TEC data in the American sector. This event holds significance as it serves as a valuable reference for the study of midlatitude plasma depletions during other storms. This study addresses aspects that were not previously covered in the literature. While previous studies have discussed EPB-related aspects of this event (Aa et al., 2019; Zakharenkova & Cherniak, 2020), our investigation focuses on non-EPB aspects to provide a more balanced understanding of this phenomenon.

2. Observational Data

This study utilizes two data sets: the GNSS TEC data obtained from the Coupling, Energetics, and Dynamics of Atmospheric Regions (CEDAR) Madrigal database (http://cedar.openmadrigal.org/index.html/) and zonal plasma velocity measurements collected by digisondes from the Global Ionospheric Radio Observatory (GIRO) (https://giro.uml.edu/) (Reinisch & Galkin, 2011). The GNSS TEC data is utilized to create TEC maps and keograms. To reduce data gaps in low latitudes, we opted for 15-min resolution TEC maps, although 30-s resolution TEC data are available. Additionally, we generated detrended TEC maps by subtracting background values using a 60-min running window to examine ionospheric perturbations over the US. Due to the abundant GNSS data over the US, we employed 5-min resolution detrended TEC maps. The spatial resolution for all TEC maps is set at 0.5° in both latitude and longitude. This study uses the zonal plasma velocity measurements from three digisonde stations in the American sector: Eglin (30.5°N, 86.5°W), Campo Grande (20.5°S, 55.0°W), and Cachoeira Paulista (23.2°S, 45.8°W). The data cadence at Eglin is 15 min, while at the other stations, it is 10 min. The observations at Eglin represent plasma motion at midlatitudes, and the observations at the other two stations represent plasma motion near the magnetic equator.

3. Results and Discussion

EPBs develop from the magnetic equator and extend to higher latitudes as they grow vertically (Huba et al., 2008; Kil et al., 2009; Yokoyama, 2017). Naturally, the emergence of an EPB at higher latitudes is delayed compared to its emergence at the magnetic equator due to its growth time. We first investigate this property using the TEC maps around the emergence time of the TEC depletion band.

Figure 1a presents auroral index (AE), interplanetary magnetic field (IMF), and symmetric magnetic perturbation index (SYM-H) on 7–8 September 2017. Following the southward turn of the IMF, the AE index increases, and the SYM-H index turns negative. The minimum SYM-H index reaches its lowest value of −146 nT at 01:08 universal time (UT) on the 8th. The global structure of the TEC depletion band was most pronounced around the time of the SYM-H minimum. The detrended TEC maps at 23:30–23:35 and 01:00–01:05 UT in Figures 1b and 1c show the development of complex ionospheric perturbations in the Eastern US before and during the development of the TEC depletion band. Figures 1d–1f are the TEC maps at 23:30–23:45, 23:45–00:00, and 00:45–01:00 UT, respectively. In the TEC map at 23:30–23:45 UT (Figure 1d), notable TEC perturbations are not evident at any latitudes. We further examined the emergence time of perturbations using higher temporal resolution TEC maps because the absence of perturbations could be due to the use of a 15-min average. In 5-min resolution TEC maps, EPB signatures emerged at 23:40 UT around 70°W in the equatorial region. Previous studies (Aa et al., 2019; Zakharenkova & Cherniak, 2020) also indicate the emergence of this EPB feature around the same time in this region. We explored EPB emergence time over South America by examining digisonde data. The emergence times of spread F at five digisonde stations listed in GIRO are as follows: Fortaleza (38.4°W, 3.90°S): 23:00 UT (20:26 LT), São Luís (44.2°W, 2.6°S): 22:50 UT (19:53 LT), Cachoeira Paulista (45°W, 22.7°S): 00:00 UT (21:00 LT), Santa Maria (53.7°W, 29.7°S): 23:36 UT (20:01 LT), and Campo Grande (55.0°W, 20.5°S): 00:00 UT (20:20 LT). The earliest emergence time of spread F is 22:50 UT at São Luís, but this station is located more than 20° east of the TEC depletion band. Because stations are located at different longitudes, LT is a relevant parameter for assessing the anomality in EPB occurrence over South America. The digisonde observations suggest the development of spread F at the typical EPB onset time (~20:00 LT) on that night.

10.1029/2024GL108334

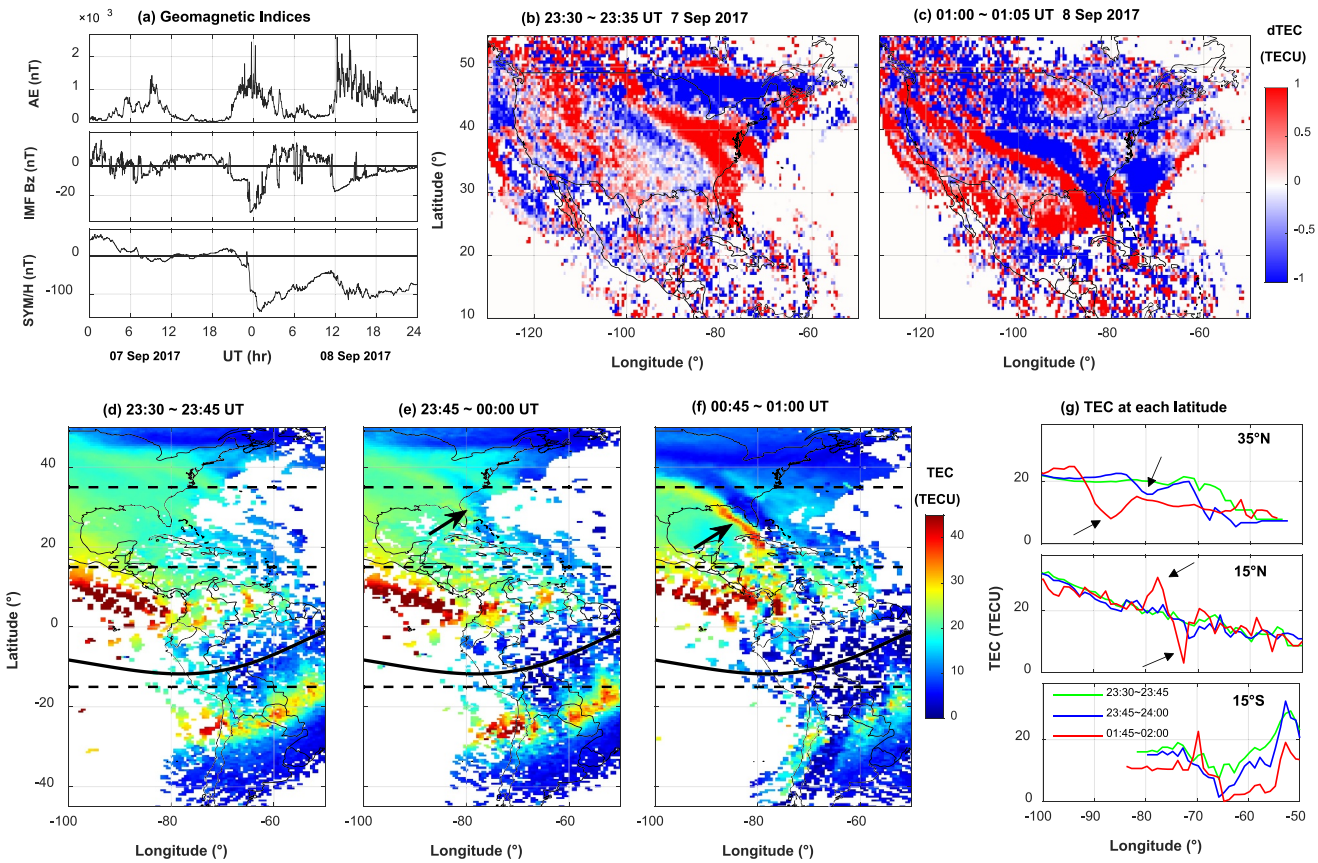

Figure 1. Emergence of a TEC depletion band in the American sector. (a) Magnetic indices. (b, c) Detrended TEC maps in North America. (d–f) TEC maps before the emergence of the TEC depletion band (23:30–23:45 UT), at the emergence of the TEC depletion band (23:45–00:00 UT), and around the time when the TEC depletion band is most pronounced (00:45–01:00 UT). (g) Longitudinal cross sections of the TEC maps at three latitudes: (top) 35°N, (middle) 15°N, and (bottom) 15°S. The data at different times are distinguished by different colors. The black arrows in the top panel indicate the locations of the TEC depletion band at 35°N.

Comparing Figures 1d and 1e, a new feature in Figure 1e is a band-like TEC depletion structure indicated by a black arrow. In Figure 1f, this feature is intensified and appear as a backward-C shape. We use the term "band" to describe the apparently elongated TEC depletion structure, but this term does not imply that the band is a single structure. Figure 1g presents the longitudinal cross sections of the TEC maps along the horizontal dashed lines at 35°N (midlatitudes), 15°N (intermediate latitude), and 15°S (equatorial region). The plots display the mean TEC values produced using the data within ±1° latitudes from the given latitudes in a 1° longitude bin. The observation times are distinguished by different colors.

We point out following aspects using the observations in Figure 1. First, the midlatitude ionosphere was perturbed before the emergence of the backward-C shaped TEC depletion band. The alignment of the perturbations in the northwest-southeast direction and their westward propagation resembles that of medium-scale traveling ionospheric disturbances. Because the TEC depletion band over the US develops in the perturbed region, it can be understood as a part of midlatitude perturbations. Second, a band-like TEC depletion structure emerged nearly simultaneously from the equatorial region extending to midlatitudes. The band-like TEC depletion structure, marked by an arrow in Figure 1e, appeared at 23:50 UT in 5-min resolution TEC maps. Therefore, the time lapse between the emergence of an EPB feature at the magnetic equator (23:40 UT) and the appearance of the band-like TEC depletion feature at midlatitudes (23:50 UT) is 10 min. The extension of an EPB from the magnetic equator over 40° of magnetic latitude within 10 min seems unrealistic. 23:50 UT corresponds to 18:50 local time (LT) at 75°W. Considering that EPBs typically develop after 19:00 LT at the magnetic equator, the occurrence of an EPB at midlatitudes at 18:50 UT is anomalous. Third, the TEC depletion is much more significant at midlatitudes than at lower latitudes in Figure 1f. In the top panel in Figure 1g, the TEC depletions indicated by arrows are about 5 (blue curve) and 10 (red curve) TECU (1 TECU = 10^{16} m^{-2}). However, the TEC depletion within the band is less

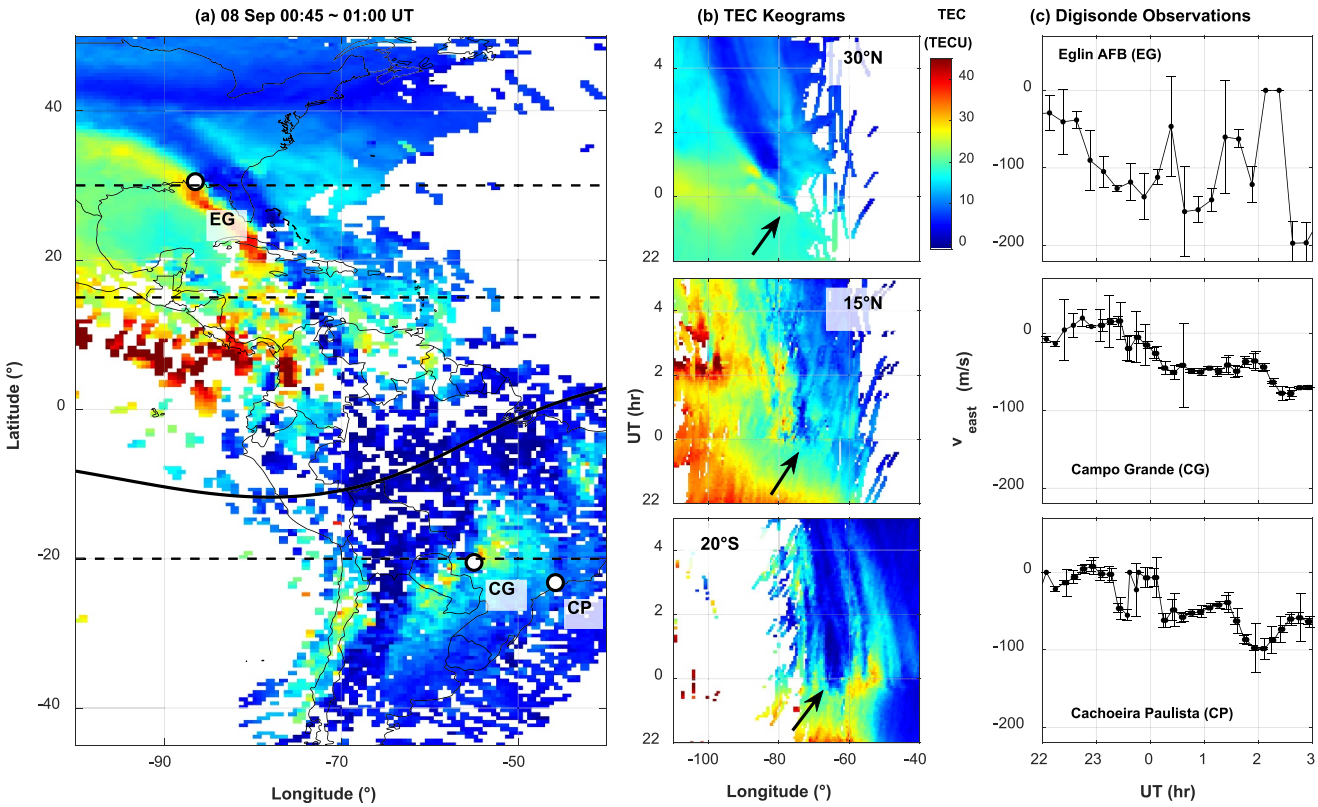

Figure 2. Evolution of the TEC depletion band at different latitudes. (a) TEC map at 00:45–01:00 with locations of three digisonde stations. (b) TEC keograms at three latitudes: (top) 30°N, (middle) 15°N, and (bottom) 20°S. (c) Zonal plasma velocity derived from the digisonde observations at (top) Eglin (EG), (middle) Campo Grande (CG), and (bottom) Cachoeira Paulista (CP). Vertical bars are standard deviations of the data.

pronounced at lower latitudes. The observations in Figures 1e and 1f depict the phenomena around sunset (19:00–20:00 LT), during which EPBs typically begin to develop and grow. It raises the question of whether an EPB can produce a more pronounced TEC depletion at higher latitudes during this period. Finally, we note the development of a band of TEC enhancement in the west of the TEC depletion band, as indicated by a black arrow in Figure 1f. The TEC enhancement is also visible in the plots at 15°N in Figure 1g, and the magnitudes of TEC enhancement and reduction (indicated by black arrows) are comparable. Thus, the TEC enhancement and depletion bands can be interpreted as paired structures associated with wave-like modulation of the ionosphere.

Based on these observations, we argue that the TEC depletion band at midlatitudes in Figure 1e is a local phenomenon independent of EPBs. The TEC depletion at this time is already about 5 TECU. This observation indicates that mechanisms other than EPBs can generate intense plasma depletions at midlatitudes. The TEC depletion at midlatitudes an hour later (Figure 1f) can be interpreted as the intensification of the existing TEC depletion by a local process or by the extension of an EPB to midlatitudes. This question is addressed later using the location of the TEC depletion at midlatitudes.

The evolution of the TEC depletion band at different latitudes is further investigated using the TEC keograms in Figure 2. Figure 2a is the TEC map at 00:45–01:00 UT. The keograms at 30°N, 15°N, and 20°S in Figure 2b are produced using the mean TEC value within ±2.5° latitudes from a given latitude in a 0.5° longitude bin. 5-min resolution TEC maps are used for the keograms. The locations of the backward-C shaped TEC depletion band are indicated by black arrows in the keograms. TEC depletion emerges just before 00:00 UT almost simultaneously at the three latitudes. It appears as a persistent structure at 30°N and 20°S, whereas it appears as a broken structure at 15°N. The different behavior at 15°N is not related to data gaps. Many data gaps also exist at 20°S, but the TEC depletion is persistent at this latitude. The broken structure may be a result of the interaction between an EPB and other perturbations or its generation by a transient process such as traveling ionospheric disturbances, yet we cannot provide a definitive answer to this question.

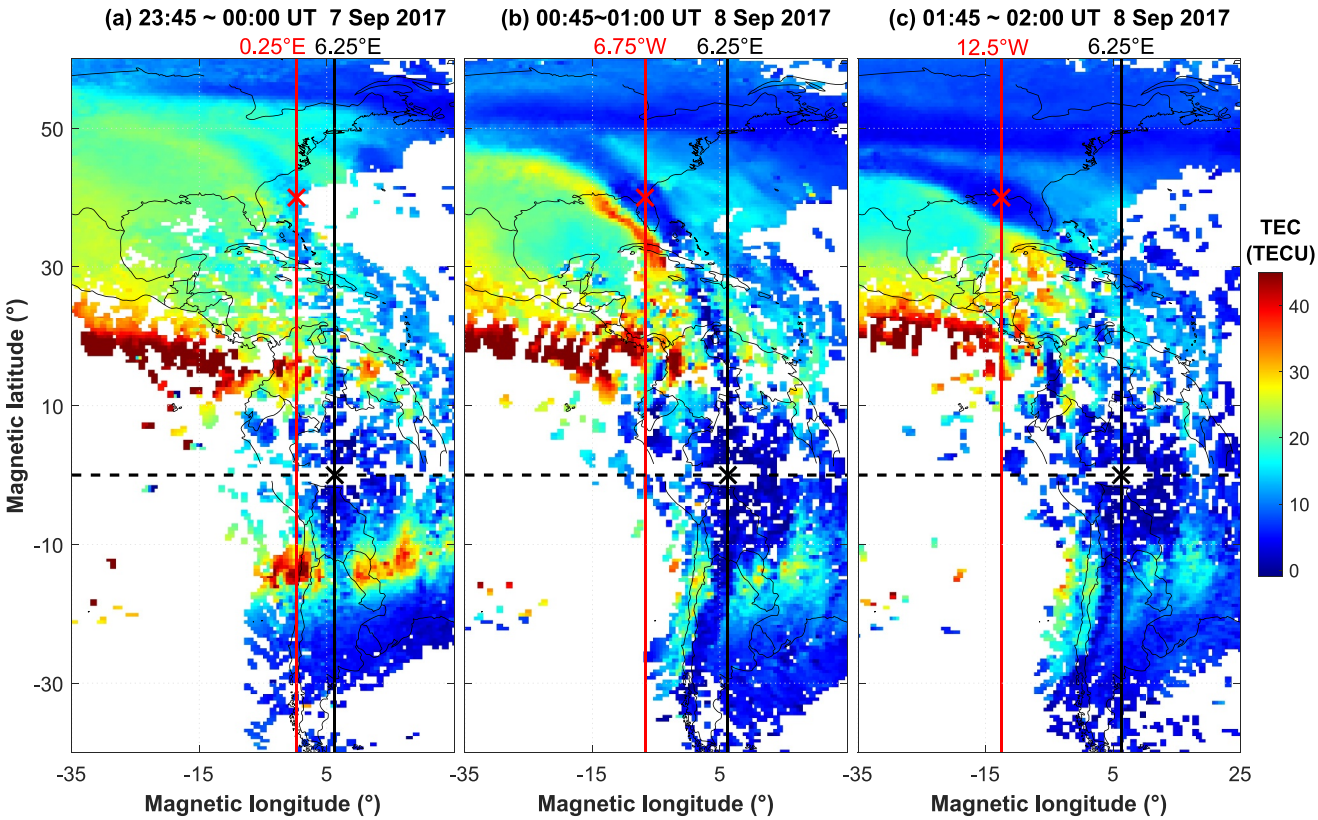

Figure 3. TEC maps in magnetic coordinates at (a) 23:45–00:00 UT, (b) 00:45–01:00 UT, and (c) 01:45–02:00 UT. The location of the TEC depletion band at the magnetic equator is indicated by a vertical black line and a black cross symbol. The vertical red line with a red cross symbol indicates the location of the TEC depletion band at 40°N.

Figure 2c shows the zonal plasma velocity derived from digisonde observations at the stations indicated by white dots in Figure 2a. The westward velocity at 30°N is greater than that at 20°S. The tilt of the TEC depletion band structure can be attributed to the latitudinal difference in the ionospheric zonal drift, but, as explained later, the tilt is seen to be too large to be explained by the difference in zonal plasma motion.

As the magnetic field lines are not parallel to the north-south direction in the American sector, we assess the tilt of the TEC depletion band using the TEC maps in the magnetic coordinates. Figure 3 shows the TEC maps in magnetic coordinates at (a) 23:45–00:00 UT, (b) 00:45–01:00 UT, and (c) 01:45–02:00 UT. Magnetic coordinates were calculated using the Altitude Adjusted Corrected GeoMagnetic model (Baker & Wing, 1989). The locations of the TEC depletion band at the magnetic equator and 40°N are indicated by the vertical black and red lines with cross symbols, respectively. The longitude (6.25°E) of the TEC depletion band at the magnetic equator is determined from the data within ±10° magnetic latitudes around 5°E at 23:45–00:00 UT. As the zonal movement of the TEC depletion band is small in the equatorial region, its location at the magnetic equator is approximated to be 6.25°E for all times.

Figure 3a shows the TEC map at the emergence time of the TEC depletion band feature. At this time, the TEC depletion band is parallel to the magnetic field lines (the vertical black line) in the equatorial region. The LT at the vertical black line is around 19:30. As post-sunset EPBs typically develop around this time (Huang et al., 2012; Kil & Heelis, 1998), the TEC depletion band in the equatorial region would be interpreted as an EPB. The TEC depletion band is also visible at 30°–45°N magnetic latitude around the vertical red line, but its location is shifted to the west about 6° from the TEC depletion band near the magnetic equator. This displacement is not explained by EPB because EPBs have just developed in the region. As well as the simultaneous emergence of TEC depletions at midlatitudes and the equatorial region, their misalignment supports our argument that the emergence of the TEC depletion band at midlatitudes is a local phenomenon independent of EPB.

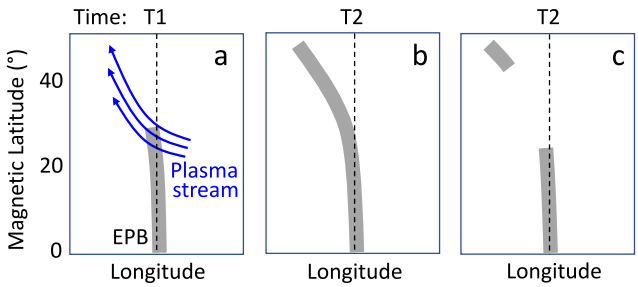

Figure 4. Schematic illustration of the impact of a plasma stream on the EPB evolution. (a) Ionospheric situations at time T1: a fully grown EPB (gray bar) extends into a plasma stream (blue arrows). (b) Anticipated EPB morphology at a later time T2 based on a previous study's hypothesis. (c) Anticipated EPB morphology at a later time T2 based on our interpretation.

Comparing the TEC depletion band at 40°N in Figures 3a and 3b, its location is shifted approximately 7° to the west, and the TEC depletion is deepened in an hour. In Figure 3b, the TEC depletion band appears as a backward-C shaped structure that extends from the magnetic equator to midlatitudes in both hemispheres. Because the time difference between these two observations is 1 hour, the intensification and displacement of the TEC depletion at midlatitudes could result from the extension of an EPB to higher latitudes in the presence of a poleward plasma stream (Zakharenkova & Cherniak, 2020). This possibility cannot be ruled out, but we are cautious in interpreting apparent TEC structures in TEC maps. For the observation in Figure 3a, we claimed that the TEC depletion band at midlatitudes is not associated with an EPB in the equatorial region, even though they apparently appeared to be an aligned structure. Similarly, the backward-C shaped structure in Figure 3b could be the combination of different structures at different latitudes.

The explanation of the entire TEC depletion band structure in terms of an EPB requires certain conditions. First, the EPB should have grown to an altitude of over 6,000 km within an hour, if transport by a plasma stream was not involved. This requires a mean vertical plasma velocity of a few kilometers per second inside the EPB. Although we lack observations to determine the magnitude and duration of the vertical plasma velocity inside the TEC depletion band, the rapid growth of an EPB to such high altitudes has not yet been demonstrated. Second, the EPB should continue to extend at midlatitudes while it decays at intermediate latitudes. When comparing Figures 3b and 3c, we can see that the TEC depletion band at midlatitudes widens and intensifies with time, but it becomes difficult to identify the band structure at intermediate latitudes in Figure 3c. Such a rapid decay of an enormously large EPB at intermediate latitudes during its growing stage raises questions. Third, the EPB should drift westward at a rate of a few hundred meters per second at midlatitudes to explain its tilt. The longitudinal distance between the TEC depletion band at the magnetic equator and 40°N is 13° in Figure 3b. If the TEC depletion at 40°N were intensified by an EPB, this EPB should have drifted westward with an average velocity of approximately 360 m/s for an hour. This velocity is 2–3 times greater than the velocity observed at Eglin (as shown in the top panel of Figure 2c). Therefore, the ionospheric motion at midlatitudes on that night does not support the connection of an EPB to the midlatitude TEC depletion.

Zakharenkova and Cherniak (2020) proposed that an EPB at low latitudes might create the observed backward-C shaped structure by being transported along with a poleward and westward plasma stream, even if the EPB did not grow to midlatitudes. Using the schematic diagrams in Figure 4, we compare their hypothesis with our own understanding of the plasma stream effect. Figure 4a depicts an EPB (gray bar) extending into a plasma stream (blue arrows) at time T1. Figure 4b represents our understanding of Zakharenkova & Cherniak's hypothesis: the transport of a section of the EPB within the stream results in a stretched EPB structure at a later time T2. However, Figure 4c portrays our understanding of the plasma stream effect: the transport of the EPB within the stream leads to its separation from the rest. An EPB can have a stretched structure, as shown in Figure 4b, when its growth persists, indicating continuous plasma depletion supply to the location where a section of the EPB is being transported. Put differently, if an EPB ceases its growth at low latitudes, the transport of a portion of it by other processes cannot produce a stretched structure extending to midlatitudes.

Figure 3d in Aa et al. (2019) shows the zonal plasma velocity around 18–19 LT in the American sector observed by Defense Meteorological Satellite Program-F17. The velocity is over 2 km/s eastward near the magnetic equator and about 600 m/s eastward around 40°N. These high velocities are inconsistent with our ground-based observations of the plasma velocity. More notably, the eastward plasma motion contradicts the behavior of the TEC depletion band, which remains stationary in the equatorial region and moves westward at midlatitudes.

4. Conclusions

The development of intense plasma depletions at midlatitudes during geomagnetic storms is explained as either the result of EPBs or local perturbations. The TEC depletion band detected in the American sector during the 8 September 2017 storm is a rare event that allows us to assess these hypotheses by tracing its evolution. The combination of the TEC depletions over the US and in the equatorial region forms a global-scale backward C-

shaped structure that resembles an EPB. Naturally, the backward C-shaped structure can be interpreted as a signature of EPBs. However, our study argues that the TEC depletion band over the US could be a local mid-latitude phenomenon. Our argument is based on the simultaneous emergence of the TEC depletion band at different latitudes, the intensification of the TEC depletion band at midlatitudes during its decay at intermediate latitudes, and the discrepancy between the TEC depletion band location at midlatitudes and the EPB location estimated by zonal plasma motion.

Taking into consideration the development of traveling ionospheric disturbance features over the US, the expansion of the high-latitude plasma convection to midlatitudes, and the formation of a steep plasma density gradient by SEDs over the US, we cannot dismiss the possibility of the TEC depletion band forming over the US in association with these phenomena. Considering the emergence of a latitudinally extended TEC depletion feature during the main phase of the storm, we can attribute the initiation of this feature to a penetration electric field, which is effective across a broad latitude. This electric field would promote the development of EPBs in the equatorial region and intensify midlatitude perturbations, resulting in the generation of a stretched TEC depletion structure along the path of the electric field. The extension of high-latitude plasma convection to lower latitudes transports the TEC depletion structure westward at midlatitudes, generating the tilted TEC depletion band observed over the US. High-speed plasma motion or polarization electric fields induced by plasma density gradients may further intensify the TEC depletion at midlatitudes, but the TEC depletion process at midlatitudes over time remains a question. The roles of various processes are challenging to elucidate through observations alone. Numerical simulations are essential to verify which process can account for the observed magnitude of plasma depletions.

Data Availability Statement

CEDAR Madrigal GNSS TEC data used for TEC maps and keograms on 7 and 8 September 2017 are available from Data-TEC1 (2024) and Data-TEC2 (2024), respectively. Plasma velocity data from Global Ionospheric Radio Observatory (GRIO) at Eglin, Campo Grande, and Cachoeira Paulista stations are available from Data-GIRO1 (2024), Data-GIRO2 (2024), and Data-GIRO3 (2024), respectively.

Acknowledgments
H. Kil acknowledges support by NSF-AGS2029840 and NASA-NNH19ZDA001N. This research in KAIST was supported by the basic research fund from Korea Astronomy and Space Science Institute (No. 2023-1-8-5018). W. K. Lee acknowledges support from the Korea Astronomy and Space Science Institute's R&D program (No. 2024190201) and the National Research Foundation of Korea (NRF) grant funded by the Ministry of Science and ICT (No. 2021M1A3A4A06099441).

References

Aa, E., Huang, W., Liu, S., Ridley, A., Zou, S., Shi, L., et al. (2018). Midlatitude plasma bubbles over China and adjacent areas during a magnetic storm on 8 September 2017. *Space Weather*, *16*(3), 321–331. https://doi.org/10.1002/2017SW001776

Aa, E., Zou, S., Ridley, A. J., Zhang, S.-R., Coster, A. J., Erickson, P. J., et al. (2019). Merging of storm time midlatitude traveling ionospheric disturbances and equatorial plasma bubbles. *Space Weather*, *17*(2), 285–298. https://doi.org/10.1029/2018SW002101

Baker, K. B., & Wing, S. (1989). A new magnetic coordinate system for conjugate studies at high latitudes. *Journal of Geophysical Research*, *94*(A7), 9139–9143. https://doi.org/10.1029/JA094iA07p09139

Chang, H., Kil, H., Sun, A. K., Zhang, S.-R., & Lee, J. (2022). Ionospheric disturbances in low- and midlatitudes during the geomagnetic storm on 26 August 2018. *Journal of Geophysical Research: Space Physics*, *127*(2), e2021JA029879. https://doi.org/10.1029/2021JA029879

Cherniak, I., & Zakharenkova, I. (2016). First observations of super plasma bubbles in Europe. *Geophysical Research Letters*, *43*(21), 11137–11145. https://doi.org/10.1002/2016GL071421

Cherniak, I., & Zakharenkova, I. (2022). Development of the storm-induced ionospheric irregularities at equatorial and middle latitudes during the 25–26 August 2018 geomagnetic storm. *Space Weather*, *20*(2), e2021SW002891. https://doi.org/10.1029/2021SW002891

Cherniak, I., Zakharenkova, I., & Sokolovsky, S. (2019). Multi-instrumental observation of storm-induced ionospheric plasma bubbles at equatorial and middle latitudes. *Journal of Geophysical Research: Space Physics*, *124*(3), 1491–1508. https://doi.org/10.1029/2018JA026309

Data-GIRO1. (2024). Zonal plasma drift velocity at Eglin station from Global Ionospheric Radio Observatory [Dataset]. *Data-GIRO1*. Retrieved %20from%20https://lgdc.uml.edu/common/DFDBYearListForStation?ursiCode=EG931

Data-GIRO2. (2024). Zonal plasma drift velocity at Campo Grande station from Global Ionospheric Radio Observatory [Dataset]. *Data-GIRO2*. Retrieved from https://lgdc.uml.edu/common/DFDBYearListForStation?ursiCode=CGK21

Data-GIRO3. (2024). Zonal plasma drift velocity at Cachoeira Paulista station from Global Ionospheric Radio Observatory [Dataset]. *Data-GIRO3*. Retrieved from https://lgdc.uml.edu/common/DFDBYearListForStation?ursiCode=CAJ2M

Data-TEC1. (2024). Total electron content data on 7 September 2017 from CEDAR Madrigal [Dataset]. *Data-TEC1*. Retrieved from https://w3id.org/cedar?experiment_list=experiments2/2017/gps/07sep17&file_list=los_20170907.004.h5

Data-TEC2. (2024). Total electron content data on 8 September 2017 from CEDAR Madrigal [Dataset]. *Data-TEC2*. Retrieved from https://w3id.org/cedar?experiment_list=experiments2/2017/gps/08sep17&file_list=los_20170908.004.h5

Huang, C.-S., de La Beaujardiere, O., Roddy, P. A., Hunton, D. E., Ballenthin, J. O., & Hairston, M. R. (2012). Generation and characteristics of equatorial plasma bubbles detected by the C/NOFS satellite near the sunset terminator. *Journal of Geophysical Research*, *117*(A11), A11313. https://doi.org/10.1029/2012JA018163

Huang, C.-S., Foster, J. C., & Sahai, Y. (2007). Significant depletions of the ionospheric plasma density at middle latitudes: A possible signature of equatorial spread F bubbles near the plasmapause. *Journal of Geophysical Research*, *112*(A5), A05315. https://doi.org/10.1029/2007JA012307

Huba, J. D., Joyce, G., & Krall, J. (2008). Three-dimensional equatorial spread F modeling. *Geophysical Research Letters*, *35*(10), L10102. https://doi.org/10.1029/2008GL033509

Kil, H., Chang, H., Lee, W. K., Paxton, L. J., Sun, A. K., & Lee, J. (2022). The origin of midlatitude plasma depletions detected during the 12 February 2000 and 29 October 2003 geomagnetic storms. *Journal of Geophysical Research: Space Physics*, *127*(3), e2021JA030169. https://doi.org/10.1029/2021JA030169

Kil, H., & Heelis, R. A. (1998). Equatorial density irregularity structures at intermediate scales and their temporal evolution. *Journal of Geophysical Research*, *103*(A3), 3969–3981. https://doi.org/10.1029/97JA03344

Kil, H., Heelis, R. A., Paxton, L. J., & Oh, S.-J. (2009). Formation of a plasma depletion shell in the equatorial ionosphere. *Journal of Geophysical Research*, *114*(A11), A11302. https://doi.org/10.1029/2009JA014369

Kil, H., Miller, E. S., Jee, G., Kwak, Y.-S., Zhang, Y., & Nishioka, M. (2016). Comment on "the night when the auroral and equatorial ionospheres converged" by Martinis, C., J. Baumgardner, M. Mendillo, J. Wroten, A. Coster, and L. Paxton. *Journal of Geophysical Research: Space Physics*, *121*(10), 10599–10607. https://doi.org/10.1002/2016JA022662

Ma, G., & Maruyama, T. (2006). A super bubble detected by dense GPS network at East Asian longitudes. *Geophysical Research Letters*, *33*(21), L21103. https://doi.org/10.1029/2006GL027512

Martinis, C., Baumgardner, J., Mendillo, M., Wroten, J., Coster, A., & Paxton, L. (2015). The night when the auroral and equatorial ionospheres converged. *Journal of Geophysical Research: Space Physics*, *120*(9), 8085–8095. https://doi.org/10.1002/2015JA021555

Nishimura, Y., Mrak, S., Semeter, J. L., Coster, A. J., Jayachandran, P. T., Groves, K. M., et al. (2021). Evolution of mid-latitude density irregularities and scintillation in North America during the 7–8 September 2017 storm. *Journal of Geophysical Research: Space Physics*, *126*(6), e2021JA029192. https://doi.org/10.1029/2021JA029192

Nishioka, M., Saito, A., & Tsugawa, T. (2009). Super-medium-scale traveling ionospheric disturbance observed at midlatitude during the geomagnetic storm on 10 November 2004. *Journal of Geophysical Research*, *114*(A7), A07310. https://doi.org/10.1029/2008JA013581

Reinisch, B. W., & Galkin, I. A. (2011). Global ionospheric radio observatory (GIRO). *Earth Planets and Space*, *63*(4), 377–381. https://doi.org/10.5047/eps.2011.03.001

Sahai, Y., Shiokawa, K., Otsuka, Y., Ihara, C., Ogawa, T., Igarashi, K., et al. (2001). Imaging observations of midlatitude ionospheric disturbances during the geomagnetic storm of February 12, 2000. *Journal of Geophysical Research*, *106*(A11), 24481–24492. https://doi.org/10.1029/2000JA900169

Sun, Y.-Y., Matsuo, T., Araujo-Pradere, E. A., & Liu, J.-Y. (2013). Ground-based GPS observation of SED-associated irregularities over CONUS. *Journal of Geophysical Research: Space Physics*, *118*(5), 2478–2489. https://doi.org/10.1029/2012JA018103

Yokoyama, T. (2017). A review on the numerical simulation of equatorial plasma bubbles toward scintillation evaluation and forecasting. *Progress in Earth and Planetary Science*, *4*(1), 37. https://doi.org/10.1186/s40645-017-0153-6

Zakharenkova, I., & Cherniak, I. (2020). When plasma streams tie up equatorial plasma irregularities with auroral ones. *Space Weather*, *18*(2), e2019SW002375. https://doi.org/10.1029/2019SW002375